IOP Conf. Series: Materials Science and Engineering **344** (2018) 012003 doi:10.1088/1757-899X/344/1/012003

Surface deformation monitoring of Sinabung volcano using multi temporal InSAR method and GIS analysis for affected area assessment

A Aditiya[14], **Y Aoki**[2] and **R D Anugrah**[3]
[1] Civil Engineering Department, The University of Tokyo, Tokyo 151-0063, Japan
[2] Earthquake Research Institute, The University of Tokyo, Tokyo 151-0063, Japan
[3] Urban Engineering Department, The University of Tokyo, Tokyo 151-0063, Japan
[4] Geospatial Information Agency of Indonesia, Jl. Raya Jakarta-Bogor Km. 46, Cibinong, Indonesia

E-mail: arif@iis.u-tokyo.ac.jp, yaoki@eri.u-tokyo.ac.jp, ranie@env.t.u-tokyo.ac.jp

Abstract. Sinabung Volcano which located in northern part of Sumatera island is part of a hundred active volcano in Indonesia. Surface deformation is detected over Sinabung Volcano and surrounded area since the first eruption in 2010 after 400 years long rest. We present multi temporal Interferometric Synthetic Aperture Radar (InSAR) time-series method of ALOS-2 L-band SAR data acquired from December 2014 to July 2017 to reveal surface deformation with high spatial resolution. The method includes focusing the SAR data, generating interferogram and phase unwrapping using SNAPHU tools. The result reveal significant deformation over Sinabung Volcano areas at rates up to 10 cm during observation period and the highest deformation occurs in western part which is trajectory of lava. We concluded the observed deformation primarily caused by volcanic activity respectively after long period of rest. In addition, Geographic Information System (GIS) analysis produces disaster affected areas of Sinabung eruption. GIS is reliable technique to estimate the impact of the hazard scenario to the exposure data and develop scenarios of disaster impacts to inform their contingency and emergency plan. The GIS results include the estimated affected area divided into 3 zones based on pyroclastic lava flow and pyroclastic fall (incandescent rock and ash). The highest impact is occurred in zone II due to many settlements are scattered in this zone. This information will be support stakeholders to take emergency preparation for disaster reduction. The continuation of this high rate of decline tends to endanger the population in next periods.

1. Introduction

Sinabung volcano which located in northern part of Sumatera island is part of a hundred active volcano in Indonesia called by ring of fire. Therefore some potential impact of disasters caused by volcano and tectonic activities are frequently occurred such as eruption, landslide and earthquake in surround area. Reported by the Center for Volcanology and Geological Hazard Mitigation (CVGHM) of Indonesia, Sinabung volcano since August 2010 showed its activities until recent days (Fig.1). It has been observed thin white smoke reaches a height of 50-1000 m from the mount. Visually and through the seismograph has been observed 1 eruption with the ash column height reaching 2000 m above the mount, leaning to the east. Observed lava falling as far as 500-1000 m to the southeast and east [1].

In order to observe the pattern of suface deformation occured in Sinabung volcano during 2014 to 2017 period, several geodetic methods such as GPS survey, InSAR, leveling, electronic istance measurement (EDM), and tiltmeter can be conducted. However various methods are available, each

[1] To whom any correspondence should be addressed.

with advantages and disadvantages in terms of cost, complexity, reliability, power requirements, sensitivity, and ease of use. The greatest advantage of InSAR method in a crisis is that their data is continuous observed to the ground without direct contact during a few to ten of days, wide area coverage and no need any instrument in the ground. Meanwhile other methods have limited coverage, need to close the object and power requirement.

Spaceborne Synthetic aperture radar (SAR) interferometry is a geodetic technique based space that provides high-resolution measurements of the ground displacement associated with various geophysical phenomenons such as earthquake [2], volcano [3] [4] [5], urban subsidence [6], landslide [7], atmospheric researches [8], ocean applications [9].In the application of volcano monitoring, InSAR technique has demonstrated its high performance to measure surface displacements in different conditions and scenarios [10]. The advanced InSAR time series processing method referred to as Small BAseline Subset (SBAS) [11] that allows studying both the spatial and temporal variability of the surface displacements. It has proven to optimize for different models of SAR signal scattering.

This study presents surface deformations due to activities of Sinabung eruption are detectable with InSAR approach and to estimate disaster affected assessment by using GIS technique. Disaster assessment aims to mitigate the impact of eruption by consider number of houses and population when a disaster occurs. The main objective this research is to obtain rates of deformation and to assess affected area to reduce risk of disaster in the term of towards civilian resilience.

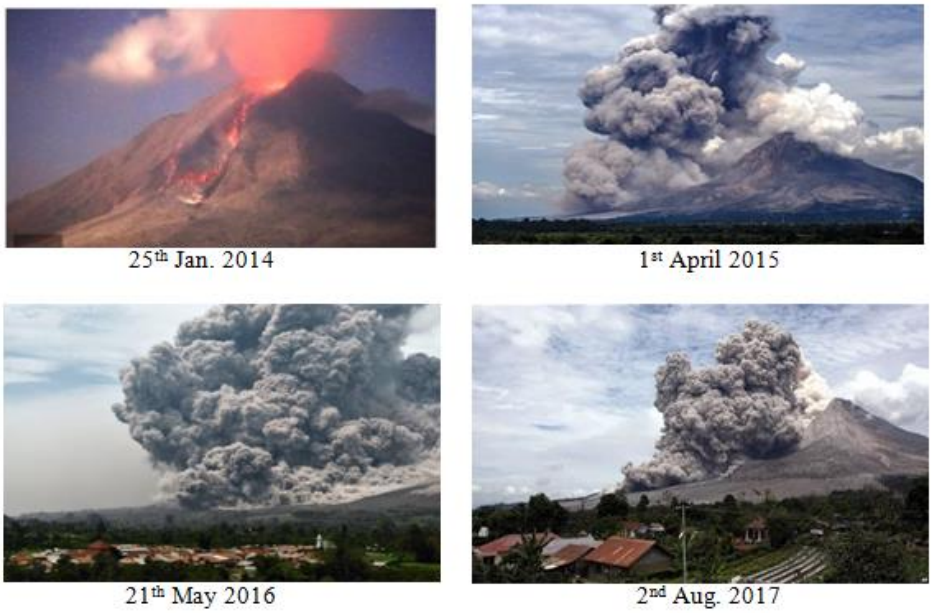

Figure 1. Recent of Sinabung eruption activities from 2014-2017

2. Methodology

2.1. Study Area and Data Sets

Sinabung volcano (2460 m) is located in the Karo plateau of Karo Regency, North Sumatra, Indonesia, 40 km from the Lake Toba supervolcano and 90 km from Medan city. The volcano was claasified as a Pleistocene-to-Holocene stratovolcano. Recent documented events include an eruption in the early hours of 29 August 2010 after long rest period 400 years ago. The first eruptions were following by

eruptions in September, November 2013, February and October 2014, April 2015, May 2016, and August 2017. According to the evacuation report, 27.671 people have been evacuated during the eruption in 2014. Therefore this study has been conducted to support local emergency response plan.

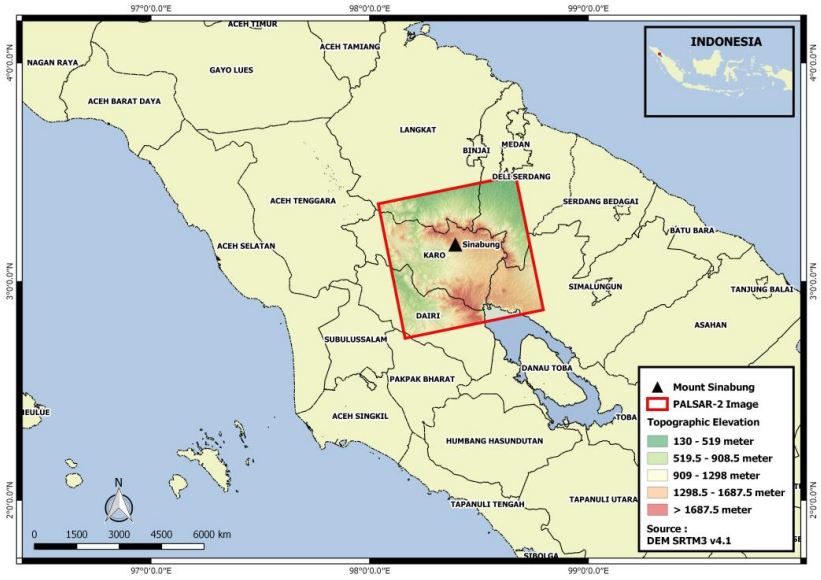

Figure 2. Geographic location of Sinabung Volcano, North Sumatera of Indonesia and red rectangle of PALSAR-2 imagery

We used the PALSAR-2 (Phased Array Type L-band Synthetic Aperture Radar) sensor onboard of the Advanced Land Observing Satellite (ALOS-2) images in this study and acquired from December 2014 to July 2017. Table 1 shows details of cover ranges PALSAR-2 data that used to observe Sinabung volcano. These data sets were acquired in the ascending orbit with an off-nadir angle 28.2°. Observation parameters for all the images were as mode Strip Map and right looking direction. All baseseline of pairs images less than 350 m , remind one pairs had a baseline of 318 m. The coherence was good performed at volcano summit and its surround, meanwhile less coherence in vegetation area.

Table 1. List of ALOS-2/PALSAR-2 data

Satellite	Orbit	$B_{PERP\ (m)}$	Track	B_{TEMP}	Nadir Angle	Acquisition Date
ALOS-2	Asc.	0 (M)	152	0	28.2°	20141202
ALOS-2	Asc.	-125.1	152	294	28.2°	20150922
ALOS-2	Asc.	-318.9	152	364	28.2°	20151201
ALOS-2	Asc.	-123.1	152	546	28.2°	20160531
ALOS-2	Asc.	0	152	588	28.2°	20160712
ALOS-2	Asc.	-4.4	152	658	28.2°	20160920
ALOS-2	Asc.	-34.6	152	798	28.2°	20170207
ALOS-2	Asc.	-258.2	152	952	28.2°	20170711

These data were used to generate interferogram and to obtain rates of surface deformation. Precise orbit data which is delivered from the product header was also used to remove the reference phase from the differential interferograms. A Shuttle Radar Topography Mission (SRTM) version 4.1 was employed to eliminate the topographic phase.

2.2. Multi-temporal InSAR

SAR is microwave remote sensing technique using at least two or more images acquired at different times to generate displacement maps to detect surface changes over a specific area. Furthermore multi temporal InSAR is advanced methods involving the parallel processing of several SAR acquisitions in time increase **[12]**. In the interferometric SAR data processing, the interferograms are generated by combining two complex SAR images **[13]**. InSAR measures the change in path length in the satellite line-of-sight (LOS) between observations. Generally for InSAR approach two SAR images from slightly different orbit configurations and at different times are combined to exploit the phase difference of the signals LOS (line of sight). By assuming that the scattering phase is the same in both images, the interferometric phase ϕ is a very sensitive measure of the range difference R_2 - R_1 i.e :

$$\boldsymbol{\phi = \phi_1 - \phi_2 = \frac{4\pi}{\lambda}\ (R2 - R1)}$$

Here, ϕ_1 and ϕ_2 are the phases of the first and second SAR images, respectively; R_1 is the distance from the SAR to the scatterer by the first acquisition; R_2 is the distance by the second acquisition; and , λ is the wavelength, as for L-band ALOS-2 data λ is 23.6 cm. Many factors contribute to changes in path length, but with appropriate removal of topographic effects, and if atmospheric and ionospheric effects are small and/or can be isolated, path length changes correspond to deformation of the Earth's surface. It can be expressed as below.

$$\phi_{int} = \phi_{topo} + \phi_{defo} + \phi_{orb} + \phi_{atm} + \phi_{scatt} + \phi_{noise}$$

where ϕ_{int} is interferometric phase, ϕ_{topo} is topographic phase, ϕ_{defo} is deformation phase due to the deformation in the radar line of slight, ϕ_{orb} is deterministic flat earth phase and the residual phase signal due to orbit in determination, ϕ_{atm} is atmospheric phase, ϕ_{scatt} is phase due to a temporal and spatial change in the scatter characteristics of the earth surface between the two observation times, and ϕ_{noise} is phase degradation factors, caused by e.g., thermal noise, coregistration noise and interpolation noise. We applied SBAS method on an appropriate combination of differential interferograms produced by data pairs characterized by a small orbital separation (baseline) in order to reduce the spatial decorrelation phenomena [11]. Cumulative phase can be obtained by solving a linear least squares problem. However, this can produce different subsets of InSAR pairs connected in time and separated by large baselines. SBAS method allow to obtain surface deformation and to analyze their space time characteristics.

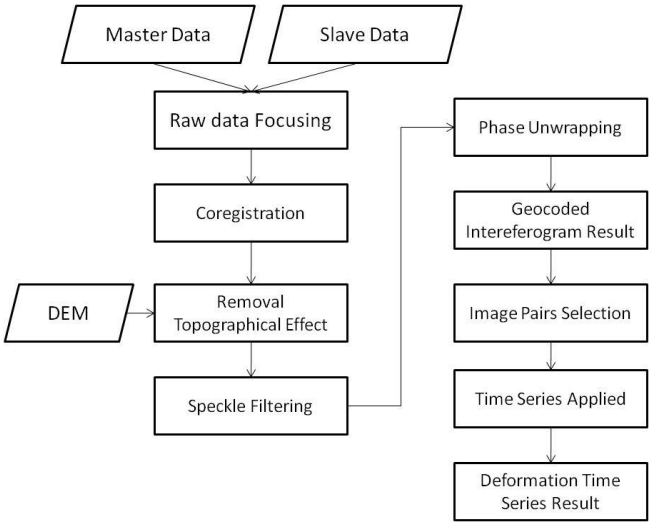

Figure 2. Processing Diagram of multi temporal InSAR

2.3. GIS Assessment

Geographic Information System (GIS) technique is a set of tools in a computer based information system that can store, retrieve, create a model, manipulate, transform, analyse, share, and display the data which are referenced to the Earth spatially for a specific purpose [14]. One of the most important application of GIS for disaster is establishing data and analytical modelling, support the decision making for pre-impact planning, post event response, and the mitigation process [15]. GIS applied to identify and prioritize the prone area to volcano hazard in Sinabung area, North Sumatera province. In this assessment, two types of data are used: (1) hazard data defined as disaster prone areas of Sinabung volcano, and (2) exposure data defined as the number of building and population.

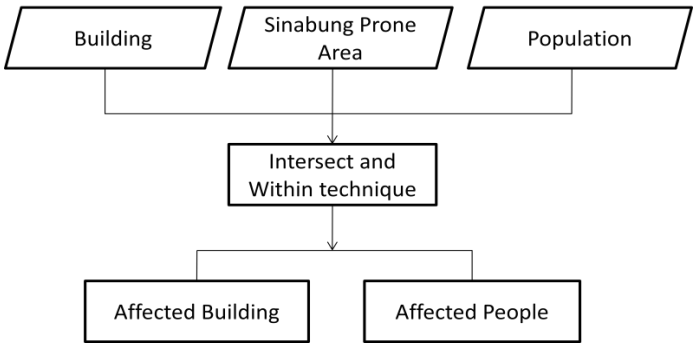

Figure 3. Diagram of GIS technique for Affected Disaster Estimation

The hazard data obtained from National Agency for Disaster Management (BNPB) which is divided into 3 levels of disaster vulnerability from high to low namely (1) disaster prone area 3 is a very potential area affected by hot clouds, lava flows, lava falling, stone pouring, and poisonous gas, (2) disaster prone area 2 is a potential area of hot clouds, lava flows, stones and lava storms, heavy ash rains, hot mud, lava flows, and toxic gases; and (3) disaster prone areas 1 is a potentially lava-stricken area, crushed material fall in the form of rain ash, and water with high acidity. While the exposure data

obtained from OpenStreetMap for building and population from WorldPop which open population data for almost all of Africa, Asia and America with high resolution data approximately 100 m cell size. In addition each data layer between hazard and building/population is processed using overlay technique (intersect and within tool) in GIS tools [16] and the number of affected buildings and the number of affected populations based on the level of disaster prone areas of Sinabung and visualized into the map.

3. Result and Discussion

We generated 28 interferograms and processed time series data for a few points of Sinabung volcano by using GIAnT program [17]. Thereafter we computed all interferograms and the wrapped phase was corrected for spatially-uncorrelated look angle error and noise associated with the master image. Small Baseline Subset (SBAS) technique [11] was employed to reduce spatial decorrelation. Atmospheric artifacts are reduced through spatial-temporal filtering after the mean deformation is obtained. Iterative processing can further improve the time-series deformation estimates. By using this algorithm each deformation according to time period is able to calculate more precisely by minimizing all error components.

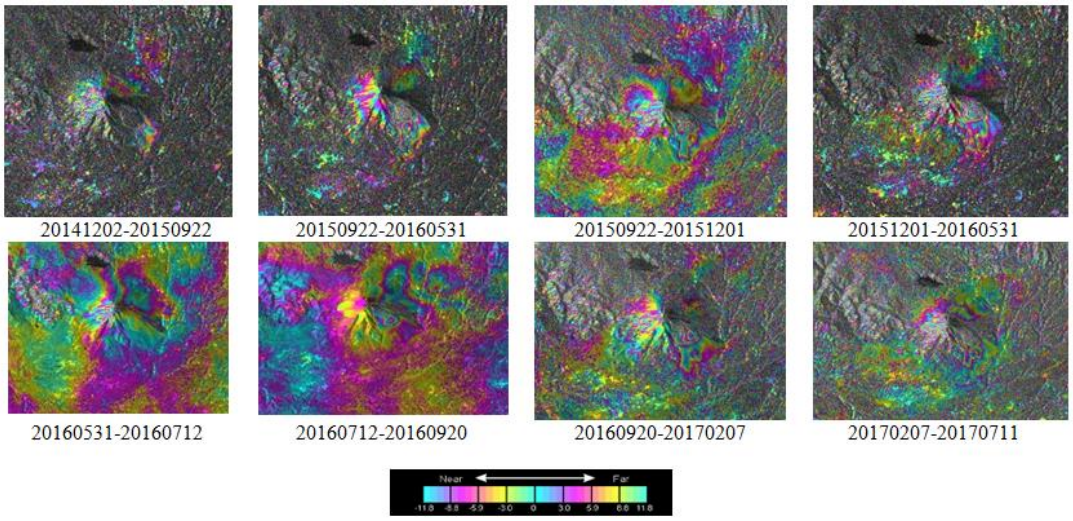

Figure 4. Interferograms of Sinabung volcano

Figure 5 shows point A and B were located in western part of Sinabung summit have been surface deformation during obervation period. The surface deformation in point A and B reach up to 6-7 cm/ year. Meanwhile point C which is located in northern of Sinabung summit has small deformation 1.9 cm/ year and point D 0.8 cm/ year. Point G has significant deformed up to 16 cm in almost 3 years and followed by point F where is near Sinabung summit approximately 9 cm.

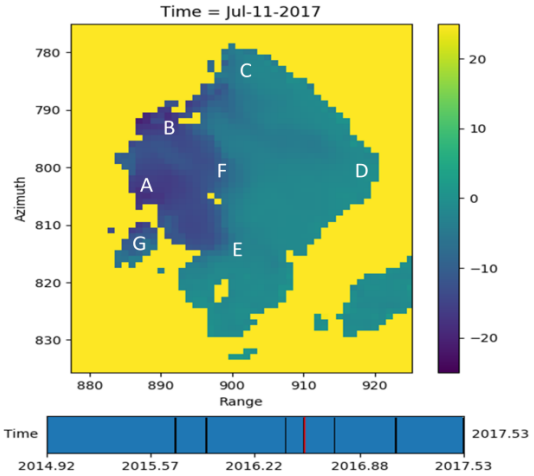

Figure 5. Observation Point at Sinabung Volcano

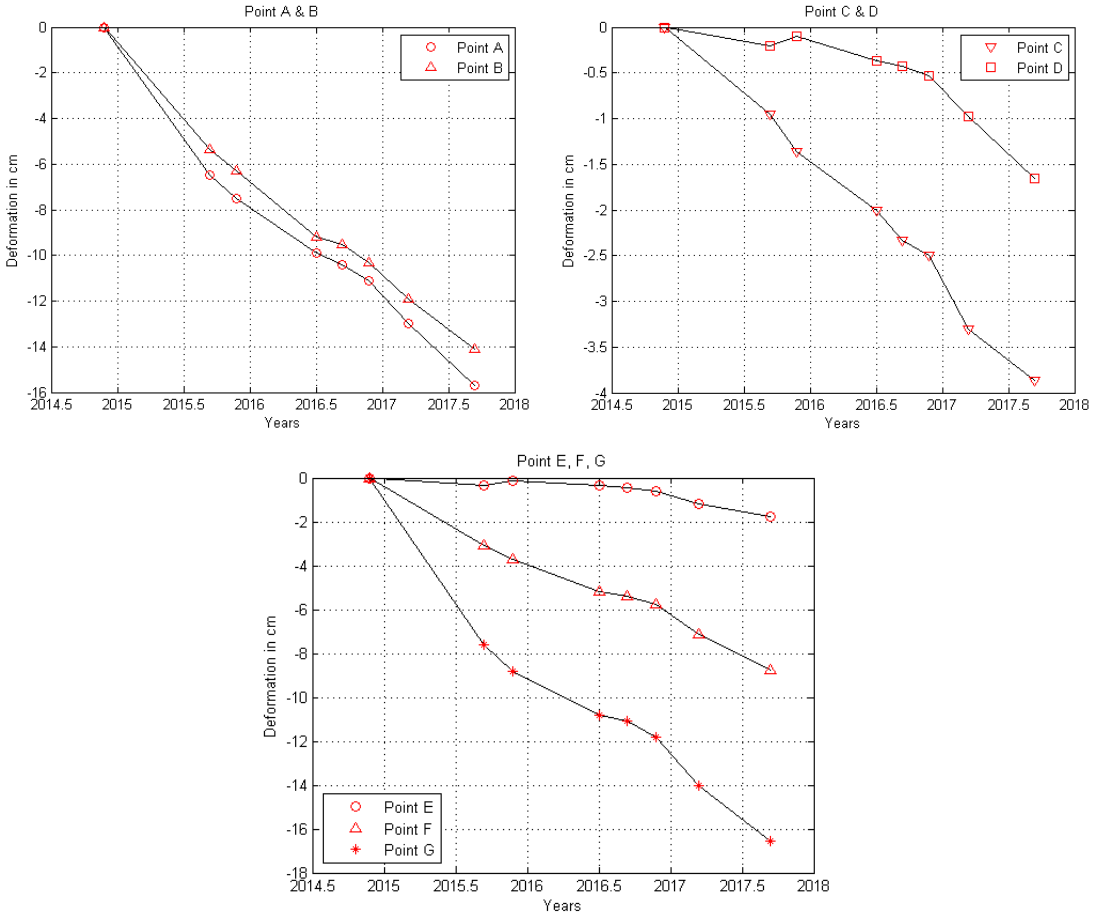

Figure 6. Time Series InSAR Result

The deformation was likely due to the deflation of magma from a deep source to the shallow reservoir. This phenomenon may have been caused by the deppressurization of the magma chamber due to periodic volcanic degassing at the Sinabung summit.

In term of disaster management GIS is used to support pre-impact planning, post event response, and the mitigation process. There are two types of output that are made such as a map showing the number of buildings affected and population affected by the eruption of Sinabung volcano based on the level of disaster prone area. This information could be used as reference for the development of volcano mitigation plans in reducing the damages and losses. It could be used to improve awareness and preparedness of the community, especially those located in volcano prone areas. Table 2 shows the number of buildings and affected persons in prone areas 1, 2 and 3. The disaster-prone area 2 has potential to suffer huge losses due to the large number of residents who live and the number of building affected by eruption.

Table 2. The Estimation Results of Buildings and Populations affected by the eruption of Sinabung

Disaster Zone	Building affected	People affected
Disaster prone area 3	4800	7600
Disaster prone area 2	5700	7100
Disaster prone area 1	1100	1500
Total	11,600	16,200

The total buildings were affected by 11,600 buildings and the highest number of affected buildings were in disaster prone areas 2 as many as 5700 buildings. While total people were affected by 16,200 people and the highest number of affected population is in disaster prone areas 3 as many as 7600 people, then the lowest number of affected population is in disaster prone areas 1 as many as 1600 people. This is because that in disaster prone areas 2 and 3 is a residential area with high population. The following is a table showing the estimated number of buildings and populations affected.

Figure 7 shows the map of buildings and people affected of Sinabung eruption based on criteria refers to the National Disaster Management Agency. This method directly related to the geographical conditions, social and economic communities living around the volcano. By adopted the result obtained from this method can be mitigate disaster impact.

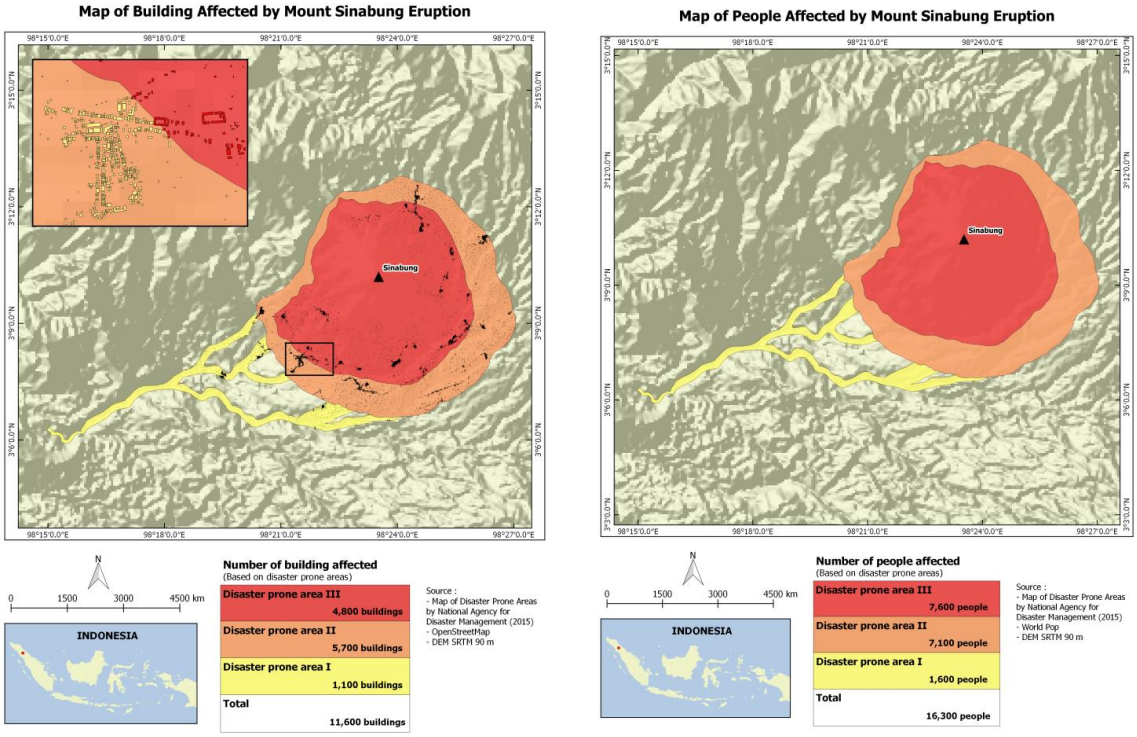

Figure 7. GIS Result of Building (left) and People Affected (right)

4. Conclusion

This work has presented an analysis of the surface deformation phenomena in Sinabung volcano. The advanced multi-temporal InSAR technique has been applied to this site by using eight PALSAR-2 images acquired from December 2014 to July 2017. We identified a few locations have deformed rates up to 15 cm during observation period. The average subsidence velocity map has been retrieved by Small Baseline approach to reduce spatial decorrelation characteristics among image itself. A rapid period of surface defromation occured during the 2,5 years of the post-eruption period. The greatest surface deformation was measured up to 6-7 cm/ year at the western part of Sinabung summit. We concluded the observed deformation primarily caused by volcanic activity respectively after long period of rest. The surface deformation at Sinabung volcano was correlated greater locally. There could also be possible existence of other causes due to geological factors in almost all deformation areas such as tectonic processes in Sumatra island. Future investigation can improve the findings of this study by utilizing other techniques. In addition the results of GIS analysis show that disaster-prone area 2 has potential to suffer huge losses than disaster prone area 1 and 3 due to the large number of population and building affected by eruption. This information could be used by local government and stake holders to mitigate disaster impact and people evacuation needed.

Acknowledgement

We thank to Indonesia Endowment Fund for Education (LPDP) for financial study support. These data were made available by PALSAR Interferometry Consortium to Study our Evolving Land surface (PIXEL) under research contract with the Earthquake Research Institute of the University of Tokyo.

References

[1] CVGHM. (2017, August) Magma Indonesia. [Online]. https://magma.vsi.esdm.go.id/

[2] D. Massonnet et al., "The displacement field of the Landers earthquake mapped by Radar interferometry," *Nature*, pp. 138-142, 1993.

[3] Y. Aoki and T. P. Sidiq, "Ground deformation associated with the eruption of Lumpur Sidoarjo mud volcano, east Java, Indonesia," *Journal of Volcanology and Geothermal Research*, pp. 96-102, 2014.

[4] Y. Aoki, "Space Geodetic Tools Provide Early Warnings for Earthquakes and Volcanic Eruptions," *J. Geophys. Res.*, pp. 3241-3244, April 2014.

[5] E. Chaussard, F. Amelung, and Y. Aoki, "Characterization of open and closed volcanic systems in Indonesia and Mexico using InSAR time series," *J. Geophys. Res. Solid Earth*, vol. 118, pp. 3957–3969, 2013.

[6] Estelle Chaussard, Falk Amelung, Hasanudin Abidin, and Sang-Hoon Hong, "Sinking cities in Indonesia: ALOS PALSAR detects rapid subsidence due to groundwater and gas extraction," *Remote Sensing of Environment*, vol. 128, pp. 150-161, 2013.

[7] Romy Schlögel, Cécile Doubre, Jean-Philippe Malet, and Frédéric Masson, "Landslide deformation monitoring with ALOS/PALSAR imagery : A D-InSAR geomorphological interpretation method," *Geomorphology*, pp. 314-330, 2014.

[8] Michael Jehle and David Small, "Measurement of Ionospheric TEC in Spaceborne SAR Data," *IEEE Transactions on Geoscience and Remote Sensing*, vol. 48, pp. 2460-2468, June 2010.

[9] Rudi Gens, "Oceanographic Applications of SAR Remote Sensing," *GIScience & Remote Sensing*, vol. 45, no. 3, pp. 275-305, 2008.

[10] Yan Zhan and Patricia M. Gregg, "Data Assimilation Strategies for Volcano Geodesy," *J. Volcanol. Geotherm. Res.*, 2017.

[11] Paolo Berardino, Gianfranco Fornaro, Riccardo Lanari, and Eugenio Sansosti, "A New Algorithm for Surface Deformation Monitoring Based on Small Baseline Differential SAR Interferograms," *IEEE Transactions on Geoscience and Remote Sensing*, pp. 2375-2382, 2002.

[12] A. Hooper, "A Mutli-temporal InSAR Method Incorporating both Persistent Scatterer and Small Baseline Approaches," *Gephys. Res. Lett.*, vol. 35, 2008.

[13] R F Hanssen, *Radar Interferometry : Data Interpretation and Error Analysis*. Dordrecht: Kluwer Academic, 2001.

[14] I. Heywood, S. Cornelius, and S Carver, *An introduction to geographical information systems*.: Pearson Prentice Hall, 2006.

[15] K. Chen, R. Blong, and C. Jacobson, "Towards integrated approach to natural hazard risk assessment using GIS: With references bushfires," *Environmental Management*, pp. 546-560, 2003.

[16] I. R. Pranantyo, M. Fadmastuti, and F. Chandra, "InaSAFE Applications in Disaster Preparedness," in *4th International Symposium on Earthquake and Disaster Mitigation 2014 (ISEDM 2014)*, Bandung, 2015.

[17] P. S. Agram et al., "New Radar Interferometric Time Series Analysis Toolbox Released," *Eos Trans. AGU*, vol. 97, no. 7, pp. 69-70, February 2013.